Heterogeneous & Homogeneous & Bio- & Nano-

CHEMCATCHEM

CATALYSIS

Accepted Article

Title: Efficient liquid-assisted grinding selective aqueous oxidation of sulfides using supported heteropolyacid catalysts

Authors: Valeria trombettoni, Ana Franco, A. Gabriel Sathicq, Christophe Len, Gustavo P. Romanelli, Luigi Vaccaro, and Rafael Luque

To be cited as: *ChemCatChem* 10.1002/cctc.201900296

Link to VoR: http://dx.doi.org/10.1002/cctc.201900296

A Journal of

ChemPubSoc Europe

WILEY-VCH

www.chemcatchem.org

Efficient liquid-assisted grinding selective aqueous oxidation of sulfides using supported heteropolyacid catalysts

Valeria Trombettoni [a,b], Ana Franco[a], A. Gabriel Sathicq[c], Christophe Len[d], Gustavo P. Romanelli[c], Luigi Vaccaro [b]* and Rafael Luque [a,e]*

[a] *Departamento de Química Orgánica, Universidad de Córdoba, Edificio Marie Curie (C-3), Carretera Nacional IV-A, Km 396, E14014, Córdoba, Andalucía, Spain, E-mail: rafael.luque@uco.es*

[b] *Laboratory of Green S.O.C. – Dipartimento di Chimica, biologia e Biotecnologie, Università degli Studi di Perugia, Via Elce di Sotto 8, 06123 – Perugia – IT, E-mail: luigi.vaccaro@unipg.it*

[c] *Centro de Investigación y Desarrollo en Ciencias Aplicadas "Dr. Jorge J. Ronco" (CINDECA), CCT-La Plata-CONICET, Departamento de Química, Facultad de Ciencias Exactas, Universidad Nacional de La Plata, 47◦N 257, B1900AJK La Plata, Argentina*

[d] *IRCP, UMR 8247 CNRS Chimie ParisTech11, rue Pierre et Marie Curie, F-75005 Paris, France*

[e] *Peoples Friendship University of Russia (RUDN University), 6 Miklukho-Maklaya str., 117198, Moscow, Russia*

KEYWORDS: Mechanochemistry; Oxidation; Heteropolyacids

10.1002/cctc.201900296

ABSTRACT

The present work reports the preparation of 40MoAl200 and its full characterization using a number of analytical techniques (XRD, TEM, TGA, BET, EDX). Liquid-assisted ball milling proved to be a key tool to achieve both the best efficiency of 40MoAl200 as a novel Keggin type catalyst in the selective sulfoxidation reaction and also for succeeding in its effective recovery and reuse. In addition, the liquid assisted grinding process was studied in detail evaluating the influence of different parameters such as frequency of rotation (rpm), number and size of the stainless steel balls used and reaction time. The use of aqueous hydrogen peroxide is essential as water proved to exert a crucial role to improve both yields and selectivity towards sulfoxide formation. The procedure was representatively extended to a number of substrates with the possibility to extend the scope of the system to produce sulfoxides in high yields (up to 95%) and satisfactory selectivities (up to 80%). The catalyst proved to be recoverable and reusable under the optimized reaction conditions.

INTRODUCTION

Mechanochemical processes have been classified by IUPAC as a "chemical reaction induced by the direct adsorption of mechanical energy". [1] The term includes several technologies in which mechanical energy can be generated and transferred to the reactants to trigger a reactive process. In particular the ball milling exploits the mechanical energy generated by the movements of the milling balls; the size, number and material of milling balls employed are the most important parameters that influence this phenomenon.[2] Different options of ball milling movements are possible; thus shaking, mixing, vibrational or planetary movements could drastically influence the outcome of a mechanochemical transformation. One of the most relevant advantages of ball milling ("dry milling") is the possibility to work in a solventless system; under effective milling which ensures optimum contacts between solid reagents, facilitating solvent-free reactions.[3–4] Another strategy commonly put in place deals with the utilization of small amounts of solvents, to conduct "Liquid Assisted Grinding" ("LAG"); indeed in the presence of minimum quantities of reaction medium, solvent effects can be brought to the mechanochemical reaction also improving the contact among reagents. [5] Due to the properties mentioned above, ball milling is considered an engaging tool especially in a sustainable context; indeed has remarkably attracted the attention in research in recent decades. [6] Mechanochemistry is to date widely exploited in a wide range of applications in different fields including down-stream processing for plants treatment, [7] mechanical pre-treatment of lignocellulosic biomass, [8] and pharmaceutical formulation preparation. [9] Additionally, mechanochemistry has been recently extended to the synthesis of metal complexes, [10] the production of catalysts and nanomaterials [11-15] and the formation of metal-organic frameworks. [16] Organic mechanochemical synthesis has also been gaining momentum in

recent years considered an important and versatile tool for the sustainable production of target organic compounds. [17-22]

Additionally, LAG has proven to be useful for a variety of transformations [23-25] confirming the many advantages of this tool compared to conventional (heating) technologies [26-27] and showing how yields of the isolated products can be improved dramatically. [28]

Despite mechanochemical oxidation reactions could potentially be regarded as unpredictably safe due to the shock-sensitive nature of many oxidants, recent research in the field has been focused on the employment of safer, easier-to-handle materials. Indeed several mechanochemical oxidation protocols are widely reported in literature in which shock-stable oxidants were employed, thus ensuring safety under mechanochemical conditions. [29-33]

In particular, this contribution is focused on sulfoxidation reaction, an important process generally focused on the selective production of alkyl, benzyl, and aryl sulfoxide compounds useful for several applications in different fields as active pharmaceutical ingredients (APIs), [34-35] ligands, [36] and flavour agents. [37] In this context, sulfoxidation reactions using mechanochemical activation have been little explored in literature. A representative example has been reported by Cravotto et al. for the desulfurization of medium/high sulfur content paraffins (up to 3000 mg/kg). The procedure was carried using Oxone® as oxidant and sulfone derivatives were selectively produced in high yields (99%) and with no trace of sulfoxide detected. [38] In the oxidation reaction of organic sulfurs, catalysts play an important role and therefore the careful tailoring of catalytic systems is crucial to achieve chemoselectivity and avoid the formation of side-products. Heterogeneous catalysts are usually preferred in order to simplify the isolation procedures and minimize waste associated to the synthetic protocol. Several methodologies have been reported in sulfoxidation reactions using a wide range of heterogeneous catalysts. Representative examples include

transition metal functionalized graphene oxide, [39] Keplerate polyoxometalates ionic liquid complexes, [40] iron oxides on carbon-based supports, [41] transition-metal oxide clusters, [42] tungsten (VI) organic complexes [43] and carbon supported polyoxometalates. [44] Among the different employed catalysts, heteropolyacids (HPA) are useful in oxidation reactions [45] due to their strong Brønsted acidity and redox properties. HPAs are polyoxometalate inorganic cages known also as Keggin type materials that possess the general formula $H_n(MX_{12}O_{40})_n$, wherein M is the central atom and X is the heteroatom attached; typically M is P or Si and X is W or Mo. The disadvantages of the use of HPA related to their solubility in organic solvent commonly used and their low surface area (< 4 m^2/g). For this reason, the development of supported HPAs is an important issue which has been extensively investigated in recent years[40, 45-49] to design advanced heterogeneous catalysts with improved surface areas (even if with low porosity). This contribution has been aimed to explore the mechanochemical LAG sulfoxidation using designed heterogeneous HPA catalysts prepared via wet impregnation of phosphomolybdic acid on CATAPAL 200, a commercial crystalline pseudoboehmite as compared to bulk HPAs. The use of boehmite as catalytic support is well reported in literature; it could be considered good support thanks to its high reactivity to the surface; indeed its surface is covered by many hydroxyl groups which make possible an easy functionalization. Moreover it possesses several advantages including low toxicity, remarkably thermal and mechanical stability and good adsorption capacity. [50-55] Herein, we report the structural features of such structure and its application in the mechanochemical LAG sulfoxidation of several organic sulfides as a representative synthetic organic application of heterogeneous catalysts under mechanochemical conditions. Hydrogen peroxide in water has been employed as ecofriendly, sustainable and cheap oxidant. [39]

EXPERIMENTAL SECTION

The reactions were carried out in a planetary ball milling Retsch-PM-100 using a 25 mL stainless steel jar. All reagents were commercially obtained and used without further purification, unless otherwise specified. Diphenyl sulfide (assay 98%), methyl phenyl sulfide (assay ≥ 99%) thioanisole (assay ≥ 99%), dibenzyl sulfide (assay ≥ 95%), 4-4' diamine diphenyl sulfide (assay 98%), 4 nitro-4' amine diphenyl sulfide (assay >99%), hydrogen peroxide solution (30% w/w in H_2O), urea peroxide solution (assay 97%), tert-butyl hydrogen peroxide solution 8 5-0/6.0 M in decane) and phosphomolybdic acid hydrate (≥ 99.99%, traces metals basis) were purchase from Sigma Aldrich. CATAPAL200® (particle size ~ 60 μm) was provided by Sasol Chemicals (USA) LLC. The reactions were monitored by GC and GC-MS, using an Agilent 6890N GC model equipped with a Supelco 2-8047-U (60m x 25m x 25μm i.d.) capillary column and an FID detector and the products were confirmed using GC (7890A)-MS (5975D inert MSD with Triple-Axis Detector) Agilent equipped with a capillary column HP-5MS (60 m x 0.32 mm), at the Research Support Service Center (SCAI) from University of Cordoba.

Catalysts characterization

XRD patterns were recorded using a Bruker D8 DISCOVER A25 diffractometer with a slit of 0.018° from 2θ=10° to 80° and counting time of 5 s per step using CuKα radiation. Textural properties of the samples were determined by N_2 physisorption using a Micromeritics ASAP 2000 automated system with the Brunauer-Emmet-Teller (BET) and the Barret-Joyner-Halenda (BJH) methods. The samples were outgassed for 24 h at 130°C under vacuum (P0 = 10−2 Pa) and then analyzed. TEM images were recorded with JEOL 1200, at the Research Support Service Center (SCAI) from Universidad de Cordoba. Samples were suspended in ethanol and deposited straight

away on a copper grid prior to analysis. EDX analysis were performed in a JEOL-SEM JSM-6610 LV scanning microscope in backscattered electron mode at 3/15 kV fitted with elemental analysis. ICP-MS analysis were conducted in a Philips PU 70000 sequential spectrometer equipped with an Echelle monochromator (0.0075 nm resolution). Samples were digested in HF: HNO_3: HCl (1:1:1) and subsequently analyzed at the SCAI of Universidad de Cordoba. TGA measurements were performed using a System Setaram Setsys 12 TGA instrument. Samples were heated at a heating rate of 10 ºC min^{-1}, in Nitrogen (50 mL min-1) at the temperature range 30-800 ºC. Pyridine (PY) and 2,6-dimethylpyridine (DMPY) titration experiments were carried out at 300 °C, via gas phase adsorption of the basic probe molecules applying a pulse chromatographic titration methodology. The catalyst used (≈0.025 g) was fixed inside a tubular stainless steel microreactor (4 mm internal diameter) by Pyrex glass wool. A cyclohexane solution of titrant (0.989 M in PY and 0.686 M in DMPY, respectively) was injected into a gas chromatograph through a microreactor in which the catalyst was previously sited. The injected base was analyzed by gas chromatography with a flame ionization detector and using an analytical column of 0.5 m length, containing 5 wt % of polyphenylether in the Chromosorb AW-DMCS in 80/100. The quantity of probe molecule adsorbed by the solid acid catalyst can subsequently be easily quantified. In order to distinguish between Lewis and Brønsted acidity, it was assumed that all DMPY selectively titrates Brønsted sites (methyl groups hinder coordination of nitrogen atoms with Lewis acid sites) while PY titrates both Brønsted and Lewis acid sites in the materials. Thus, the difference between the amounts of PY (total acidity) and DMPY (Brønsted acidity) adsorbed should correspond to Lewis acidity in the materials.

Preparation of 10,20,30,40 MoAl200

Four different HPA supported catalysts having different content of phosphomolybdic acid were prepared via wet impregnation method over CATAPAL 200. The procedure for the preparation of 40MoAl200 was performed in a round bottomed-flask equipped with a magnetic stirrer where 1 g of phosphomolybdic acid hydrate was dissolved in 50 mL of acetone and 2.5 g of CATAPAL 200 were slowly added. The mixture was stirred at r.t. for 10 min, followed by solvent removal by rotary evaporator. The synthesized catalyst was dried overnight at r.t. An identical procedure was employed for the synthesis of all catalysts with the only difference in the amount of phosphomolybdic acid hydrate used; 0.25, 0.5, 0.75 g for the synthesis of 10MoAl200, 20MoAl200, 30MoAl200 respectively.

Representative mechanochemical procedure for the oxidation reactions of diphenyl sulfide (**1a**) using 40MoAl200 as catalyst: In a typical procedure 1 mmol of diphenyl sulfide (**1a**) (169 μL), 1 mmol of H_2O_2 30% (w/w) water solution (113 μL) and 0.043 mmol% of catalyst (2 mg) were laid in a 25 mL jar and eight (Ø 10 mm) stainless steel balls were employed. The planetary ball milling was carried on at 350 rpm for 15 min. The crude reaction mixture was recovered from the jar using 200 μL of toluene and the liquid phase was analyzed by GC and GC-MS using the following conditions; injector temperature 250°C, detector temperature 350°C. Gas carrier: nitrogen (1.8 mL/min), temperature program: from 120°C (4 min) to 200°C at 10°C/min. The retention times of diphenyl sulfide (**1a**), diphenyl sulfoxide (**2a**), and diphenyl sulfone (**3a**) were 8.244, 10.326, 10.659 min., respectively.

Mechanochemical procedure for synthesis of diphenyl sulfoxide (**2a**); Scaled up reaction: For the scale up of the protocol 20 mmol of diphenyl sulfide (**1a**) (3.3 mL), 20 mmol of H_2O_2 30%

(w/w) water solution (2.25 mL) and 0.043 mmol% of catalyst (40 mg) were laid in a 25 mL jar and eight (Ø 10 mm) stainless steel balls were employed. The planetary ball milling was carried on at 350 rpm for 15 min. The crude reaction mixture was recovered from the jar using 3.5 mL of Toluene. The liquid phase was dried using sodium sulfate and subsequently purified by crystallization in water methanol solution (8 mL, 3:2 water methanol). Diphenyl sulfoxide was obtained as a white solid (19.2 mmol, 3.88 g, 96% isolated yield). The product structure was further confirmed using GC-MS and NMR.

RESULTS AND DISCUSSION

Different catalysts containing varying HPA loadings were prepared by impregnating phosphomolybdic acid into CATAPAL200 [44] obtaining 10MoAl200, 20MoAl200, 30MoAl200 and 40MoAl200. The commercial support employed for this purpose (CATAPAl200) is a crystalline boehmite material exhibiting well defined features in term of surface area, pore diameter, acidity and thermal resistance as illustrated in the detailed materials characterization.

XRD studies

Diffraction XRD patterns are shown in Figure 1. The black solid line pattern corresponds to CATAPAL200 boehmite crystalline orthorhombic phase exhibiting all the characteristic peaks. [48] The impregnation of phosphomolybdic acid on CATAPAL200, illustrated for 40MoAl200 did not significantly influence the crystalline structure of the support (discontinuous red line, Figure 1). The orthorhombic structure was well retained. The crystal size of 40MoAl200 was estimated as 31.98 nm using the Scherrer equation based on the characteristic 2θ diffraction line at 28.173.

10.1002/cctc.201900296

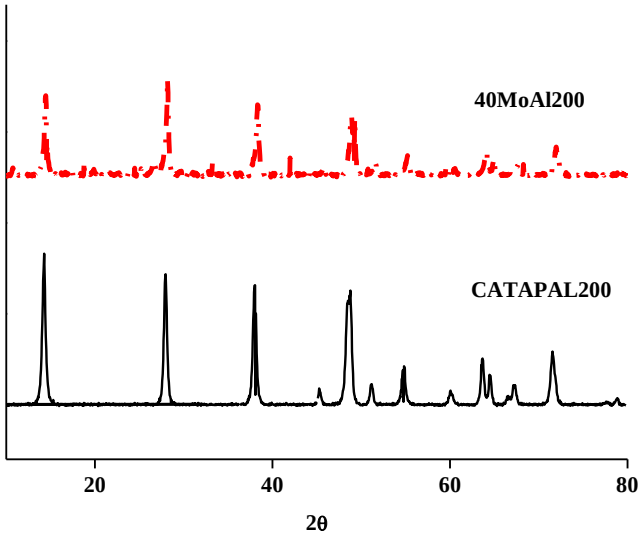

Figure 1. XRD patterns; Black solid line: CATAPAL200; Discontinuous red line: 40MoAl200.

Catalyst morphology from TEM images

TEM studies were performed to confirm XRD analyses. The images obtained from three different regions of 40MoAl200 were compared with those of the boehmite support. No morphological or structural changes could be visualized between support and impregnated material (40MoAl200 vs CATAPAL200). The boehmite phase was preserved upon impregnation, in good agreement with XRD data (Figure 2).

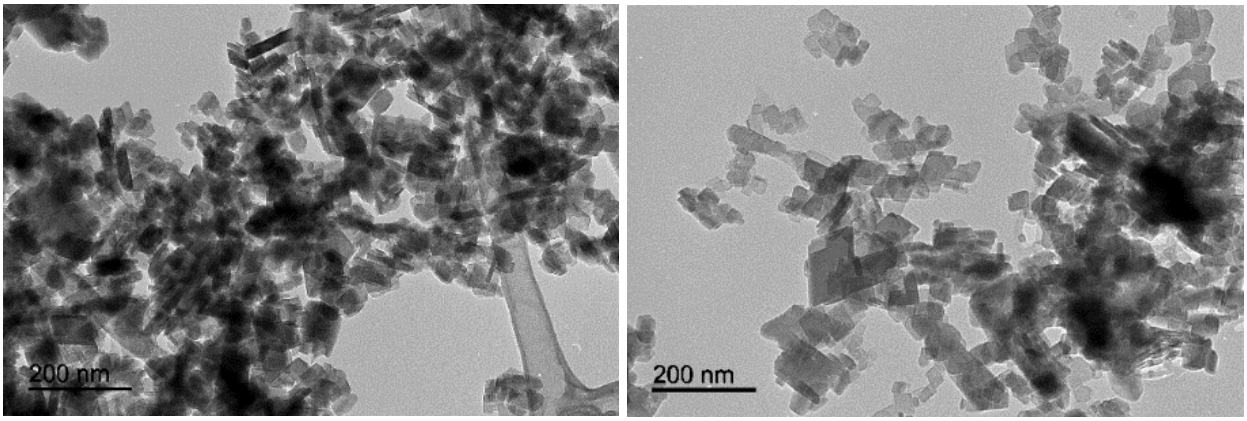

Figure 2. TEM analysis of 40MoAl200 (left panel) and TEM analysis of CATAPAL200 (right panel).

Energy dispersive x-ray spectroscopy (EDX)

EDX analysis were additionally carried on in order to demonstrate the presence of phosphomolybdic acid in the impregnated CATAPAL200 materials. Table 1 summarizes the molar percentage of all elements detected and reported as average values of three analyses on different regions of the materials. EDX analysis confirms the homogeneous presence of molybdenum and phosphorus in 40MoAl200 (Figure 3b and 3c). This information was further confirmed by ICP-MS quantitative analysis in which 26.10 ppm of Mo was detected in the material.

Table 1. EDX analysis results.

Entry	Material	Element	Intensity	%Atom [a]	%Weight [a]
1	CATAPAL 200	Al	0.87	30.0	42.0
		O	1.20	70.0	58.0
2	40MoAl200	Al	0.85	26.5	31.0
		O	0.70	68.0	47.4
		Mo	0.72	5.0	21.1
		P	0.96	0.5	0.4

[a] Average of data obtained from the analyses of three different regions of the catalysts.

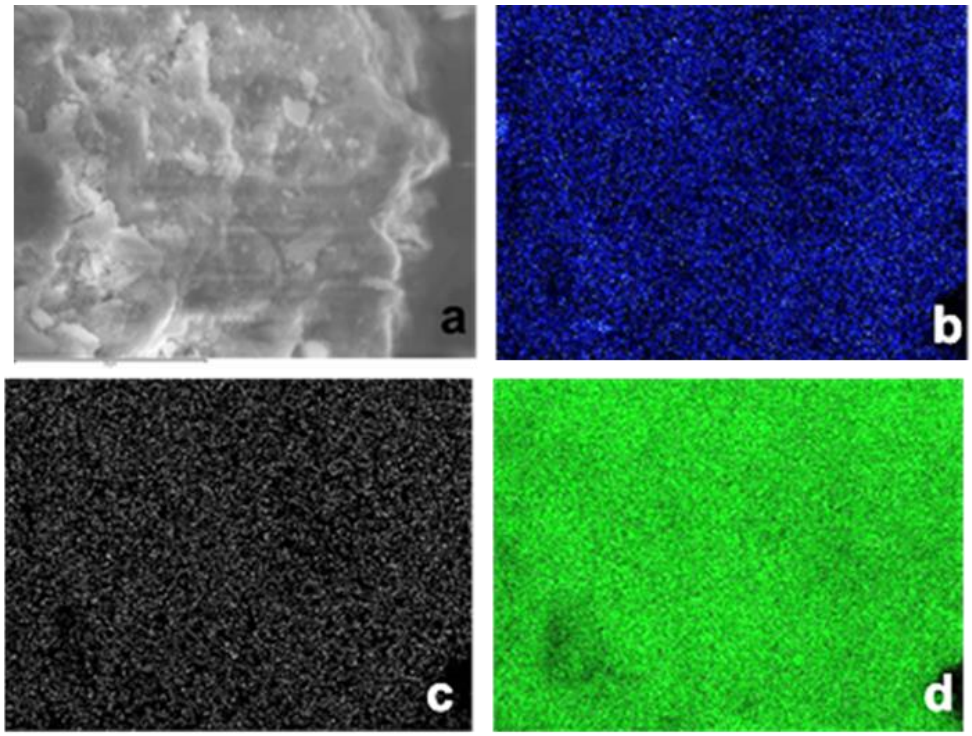

Figure 3. SEM image of 40MoAl200, b: EDS mapping of Mo, c: EDS mapping of P, d: EDS mapping of Al.

Porosimetry analysis

Figures 4a, and 4b depict the adsorption isotherm of CATAPAL200 and 40MoAl200, respectively. Type III isotherms (IUPAC classification) could be observed for both support and impregnated 40MoAl200, with a typical profile of non-porous materials (Figure 4). Indeed, the values for the Brunauer–Emmett–Teller (BET) (Table 2, entries 1 and 2) surface area and pore volumes only account for interparticular macroporosity. After HPA impregnation, a decrease of surface area was observed (from 65 to 48 m^2/g). This reduction may be attributed to the observed homogeneous dispersion of HPA within the interparticular voids.

10.1002/cctc.201900296

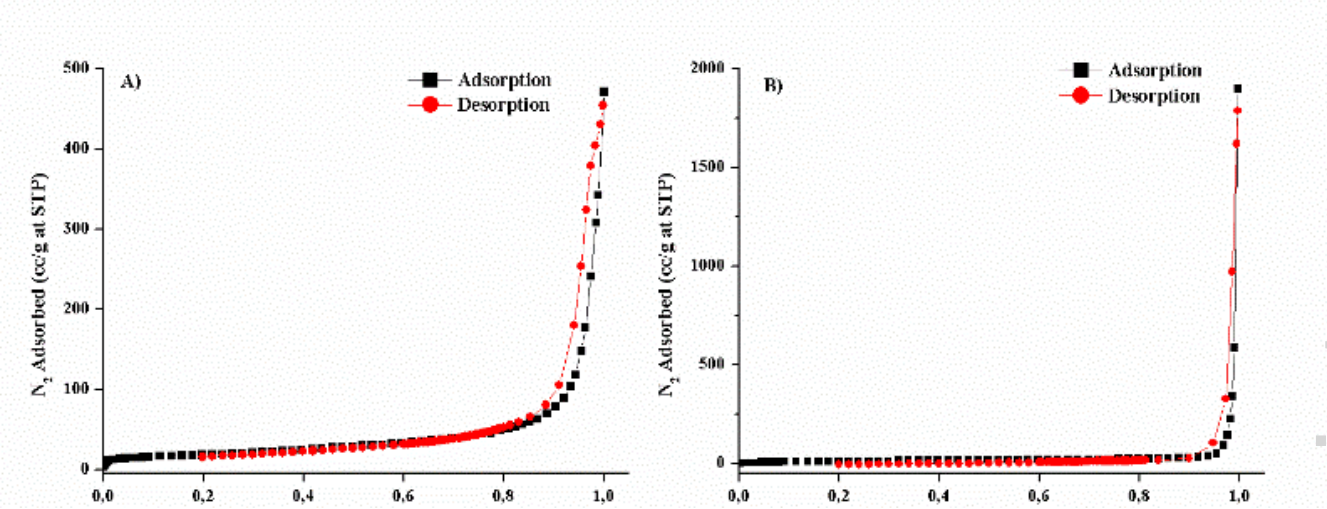

Figure 4. N_2 sorption isotherms of (a) CATAPAL200, (b) 40MoAl200.

Table 2. Textural properties of the materials prepared.

Entry	Material	S_{BET} (m^2 g^{-1}) [a]	D_{BJM} (nm)[b]	V_{BJH} (cm^3 g^{-1}) [c]
1	CATAPAL200	65	-	0.46
2	40MoAl200	48	-	0.38

[a] S_{BET}: specific surface area was calculated by the Brunauer-Emmett-Teller (BET) equation. [b] D_{BJH}: mean pore size diameter was calculated by the Barret-Joyner-Halenda (BJH) equation. [c] V_{BJH}: pore volumes were calculated by the Barret-Joyner-Halenda (BJH) equation.

Thermogravimetry analysis (TGA)

In order to evaluate the thermal stability of 40MoAl200, TGA analyses were performed. Figures 5a and b show TGA diagrams of CATAPAL200 and 40MoA200, respectively. Both of them feature three key mass losses (*black lines*). In the first one (from 0 to 100 °C) a slight weight decrease can be observed due the loss of physisorbed water. A 15% mass loss could be measured in the 400 °C to 500 °C range, in which a clear phase transition (sharp exothermic peak at ca. 520ºC) is typical from the formation a gamma-alumina phase via boehmite de (stable phase from ca. 450ºC); followed by a stable weight from 600-800°C. [53] Figure 5b depicts the TGA profile of

40MoAl200, for which a 5% of weight loss was observed from 200 °C to 400 °C, attributed to the release of water from the keggin clusters. This phenomenon is typical for Keggin type catalysts. [44] The significant mass loss (-15%) observed in the 400-500 °C similarly accounts for the observed phase transition.

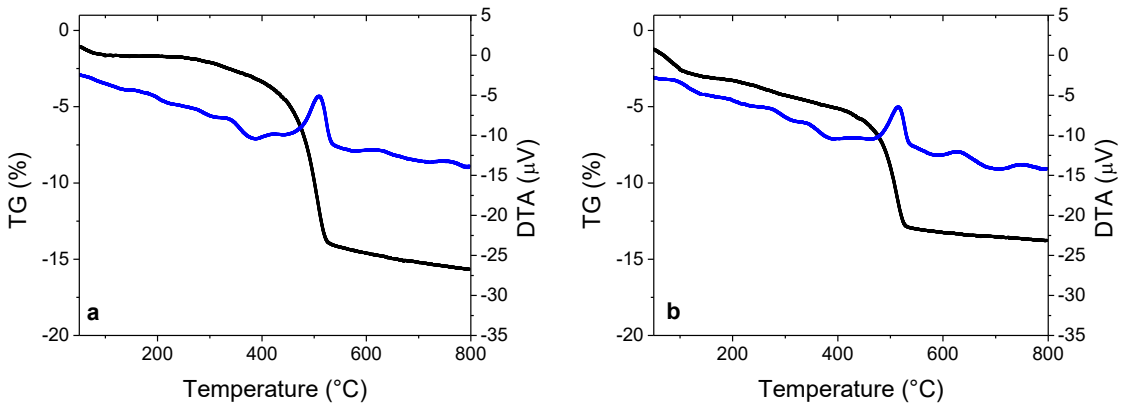

Figure 5. Thermal analysis of a: CATAPAL200, b: 40MoAl200.

Acidity of materials

The determination of the amount of acid sites and their nature (Brønsted or Lewis) was evaluated via pyridine titration. Table 3 summarizes values for both the support and the impregnated HPA materials in which a clear increase in total acidity (both Brönsted and Lewis) can be observed, confirming successful incorporation of the Keggin clusters.

Table 3. Acidity of the new materials measured by pyridine/dimethyl pyridine adsorption method.

Entry	Material	Total acidity (µmol PY/g)	Brønsted acidity (µmol DMPY/g)	Lewis acidity (µmol PY/g)
1	CATAPAL200	10	10	-
2	40MoAl200	89	53	36

Catalytic activity experiments

The investigation on the catalytic efficiency of synthesized MoAl200 catalysts (see Experimental section) was initially performed in the model oxidation of diphenyl sulfide (**1a**) to optimize the reaction conditions. Subsequently, the mechanochemical reaction was extended to a range of organic sulfides in order to define an efficient, versatile and sustainable LAG protocol (Scheme 1).

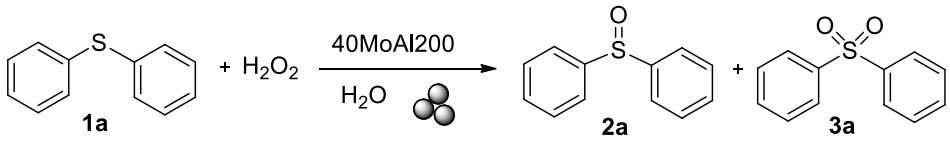

Scheme 1. General LAG protocol for the sulfoxidation of diphenyl sulfide (**1a**).

Table 4 summarizes the main results for the mechanochemical reaction for the different synthesized catalytic systems under optimized conditions. Blank runs (performed in the absence of any catalyst) gave only 8% of conversion after 15 min, confirming the essential role of the catalyst in the sulfoxidation reaction. The same result was observed when the reaction was performed in the presence of the support CATAPAL200 (Table 4, Entry 10). As it could be observed from Table 4, 40MoAl200 proved to be the best catalytic system, providing excellent results in term of conversion (95%) and selectivity (80%) towards diphenyl sulfoxide (**2a**) (Entry 2). 20MoAl200 and 10MoAl200 were less efficient allowing less than 15% conversion to **2a** and a higher selectivity towards the formation of diphenyl sulfone (**3a**) (Table 4, entries 4, 6).

Table 4. Catalytic studies of HPA supported materials in the mechanochemical oxidation of diphenyl sulphide

Entry	Catalyst (mol%)	Conversion (%)[a]	Selectivity (**2a**)/(**3a**)[b]
1	-	8	7:3
2	40MoAl200 (0.043)	95	8:2
3	30MoAl200 (0.043)	80	8.5:1.5
4	20MoAl200 (0.043)	10	3:7
5	20MoAl200 (0.430)	15	3:7
6	10MoAl200 (0.043)	5	0:10
7	10MoAl200 (0.430)	5	0:10
8[c]	40MoAl200 (0.043)	5	8.5: 0.5
9[d]	40MoAl200 (0.043)	40	8:2
10	CATAPAL200	7.5	7:3

[a]Monitored by GC analysis; [b]Determined by GC-MS analyses. Reaction conditions: 25 stainless steel mL jar containing 8 balls (Ø 10 mm),(**1a**)/ H_2O_2 1:1 molar ratio, 350 rpm, 15 min [c] 1mmol of urea-hydrogen peroxide employed as oxidant [d] 1mmol of hydrogen tert-butoxide employed as oxidant

Increasing the amounts of 20MoAl200 or 10MoAl200 did not show any improvement both in terms of conversion and selectivity (Table 4, entries 5, 7), for which these materials-together with 30MoAl200 were not further employed in any additional catalytic studies. Due to the data above reported, the catalytic activity of 40MoAl200 was further optimized under ball milling conditions.

Firstly, different oxidant agents were tested; aqueous hydrogen peroxide proved to be more efficient than urea hydrogen-peroxide and tert-butyl hydroperoxide as observed in Entries 8-9, Table 4 (see also Graph S1). The effect of catalyst loading was subsequently tested; with no relevant effect observed changing the amount of catalyst in the range of 0.043-0.172 mol% (Table 5, Entries 2-4) using 0.5 mmol H_2O_2. A slightly higher conversion to diphenyl sulfone (**3a**) was

obtained employing 2 mmol of oxidant (Entry 10-12). A slight decrease of conversion was observed, with no influence on the selectivity using just 1 equivalent of H_2O_2 at increased catalyst amounts (Entries 6-8). This can be ascribed to an insufficient contact between reagents using the minimum amount of water present in LAG (113 μL). To confirm this effect, the same reaction was performed adding 160 μL of water (0.025 M) and a >99% conversion was achieved with 83% of selectivity towards diphenyl sulfoxide (**2a**) (Table S2, entry 2). The increased amount of water improved reaction yields as it allows a better contact among the reagents suggesting that this protocol falls in the liquid assisted grinding (LAG) definition.

Table 5. Effect of the amount of catalyst in the mechanochemical oxidation of diphenyl sulfide

Entry	H_2O_2 (equivs)	40MoAl200 (mol%)	Conversion (%)[a]	Selectivity (**2a**)/(**3a**)[b]
1	0.5	/	/	/
2		0.043	50	9.3:0.7
3		0.086	58	9:1
4		0.172	60	8.8:1.2
5	1	/	8	7:3
6		0.043	95	8:2
7		0.086	50	8:2
8		0.172	65	7:3
9	2	/	15	4.5:5.5
10		0.043	>99	3:7
11		0.086	75	4:6
12		0.172	>99	2:8

[a]Monitored by GC analyses; [b] Determined by GC-MS analyses. Reaction conditions: 25 stainless steel mL jar containing 8 balls (Ø 10 mm), 350 rpm, 15 min

Additional details on the influence of the amount of oxidant over time are reported in Table S1. We also evaluated the role of the medium used both on catalytic efficiency and selectivity. Water

confirmed to give much better results compared to other solvents with varying polarity such as methanol or hexane (see Table S2, Graph S2, SI).

The effect of the milling speed in the ball mill was subsequently considered starting from previously found best conditions (25 mL stainless steel jar containing 8 balls (Ø 10 mm), (**1**)/ H_2O_2 1:1, 0.043 mol% 40MoAl200, 350 rpm, 15 min) for which diphenyl sulfoxide (**2a**) was obtained in high conversion (95%) and selectivity (80%). Figure 6 clearly depicts a lower conversion obtained when the milling speed was reduced from 350 to 150 rpm, with no relevant change in selectivity (Table S3).

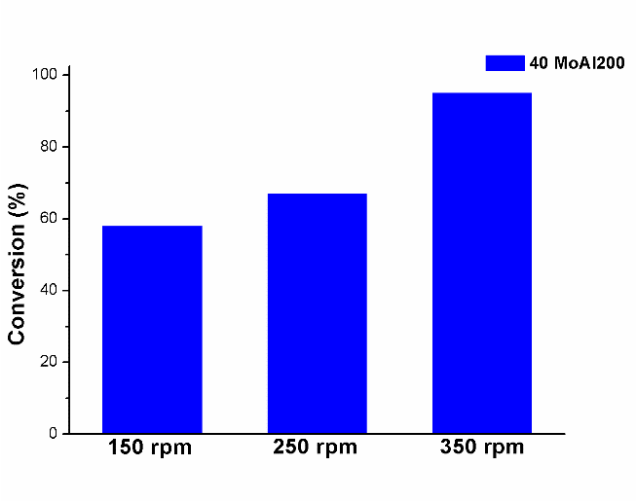

Figure 6. Effect of the milling speed in the mechanochemically LAG assisted oxidation. Reaction conditions: 25 mL stainless steel jar containing 8 balls (Ø 10 mm), (**1a**)/H_2O_2 1:1.

Another critical parameter in ball-milling experiments is the number of balls used. The experiments reported above were performed with 8 milling balls having a diameter Ø of 10 mm. The influence of this important parameter was investigated varying the number from 2 to 8 balls in the same reaction conditions. We concluded that increasing the number of balls from 2 to 8 conversion increased from 56% to 95%) in line with the increase of the internal energy system.

The selectivity to diphenyl sulfoxide (**2a**) can be improved using only 2 balls but conversion were lower even after prolonged reaction times (see Table S5 for more details).

Optimization scale-up and substrate scope

A representative scaled-up reaction of the optimised sulfoxidation of diphenyl sulfide (**1a**) was subsequently performed. The reaction was carried out using 20 mmol of diphenyl sulfide (**1a**) with a constant number and size of milled balls (8 balls, Ø 10 mm). Better results in terms of conversion and selectivity (100%, 9.95:0.05: **2a**/**3a**) were achieved as compared to smaller 1 mmol scale reactions. The satisfactory data obtained, confirmed the potential of mechanochemical reactions for large-scale applications. The isolation procedure was further optimized (see experimental section) to allow facile catalyst recovery (40MoAl200) and a 96% isolated yield of the pure product **2a** upon simple recrystallization.

Additionally, the scope of the proposed LAG mechanochemical protocol was further extended to a variety of organic sulfides **1b-e** (Scheme 2). The best conditions and results for each compound were individually optimized and the most relevant results have been summarized in Table 6. Methyl phenyl sulfide (**1c**) (Table 6, entries 3-4) proved to be very reactive, affording the preparation of the corresponding sulfoxide (**2c**) in 10 min at 99% conversion, 97% isolated yield (Table 6, entry 4). In this case, 150 rpm stirring was sufficient to provide a quantitative yield of methyl phenyl sulfoxide (**2c**) (Table 6, entry 4,). Thioanisole (**1b**) (Table 6, entry 1,2) proved to be less reactive, with a larger amount of oxidant (0.5 mmol), energy (200 rpm) and time (20 min) required to obtain (methylsulphinyl)benzene (**2d**) with satisfactory results (97% of conversion, 88% of selectivity).

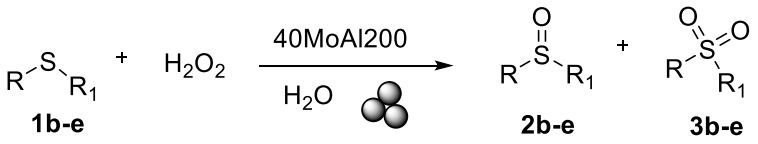

Scheme 2. "LAG" procedures to obtain organic sulfoxides **2b-e**.

Table 6. Mechanochemical oxidation of various sulphides using 40MoAl200 as catalyst

Entry	Sulfide	(**1b-e**)/ H_2O_2 molar ratio	rpm	t (min)	C (%)[a]	Selectivity **2b-e**/**3b-e**[b]
1	 **1b**	1	200	20	>99	7:3
2		0.5	350	15	97	8.8:1.2
3		0.5	350	15	>99	4.5:5.5
4	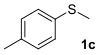 **1c**	0.25	150	10	>99	9.95:0.05
5	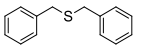 **1d**	1	200	15	98	9.9:0.1
6		2	200	15	>99	5:5
7	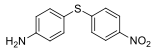 **1e**	1	350	20	10	9.8:0.2
8		2	350	20	55	5:5

[a]Monitored by GC analysis; [b] Determined by GC-MS analyses. Reaction conditions: 25 stainless steel mL jar, 0.043 %mol 40MoAl200

Benzyl sulfide (**1d**) (Table 6, entries 5 and 6) exhibited similar reactivity as compared to diphenyl sulfide (**1a**); less than 1 mmol of oxidant was not enough to obtain good results in terms of conversion and selectivity. However, (sulfinylbis(methylene))dibenzene (**2c**) could be obtained in high conversion (>99%) performing the reaction at 200 rpm for 20 minutes (Table 6, entry 6). The sulfoxidation of 4-amino-4'-nitrodiphenyl sulfide (**1d**) (Table 6, Entries 7, 8) was significantly more challenging, with only 55% conversion to 4-amino-4'-nitrodiphenyl sulfoxide (**2c**) was

detected. The reaction was less selective (ca. 50% selectivity to target product) and bis(4-nitrophenyl)sulfane was observed as reaction side-product by GC-MS. These results indicate that the oxidation of the amino group into the corresponding nitro group competed with the sulfide to sulfoxide oxidation (Supporting Information). Only traces of 4-amino-4'- nitrodiphenyl sulfone (**3d**) were found. The results obtained confirmed that the electronic nature of organic sulfides can indeed influence the LAG mechanochemical reaction in term of conversion and selectivity, [37] with electron-rich sulfides being more reactive than the electron-deficient compounds.

Catalyst stability and reusability experiments

The recovery and reuse of 40MoAl200 was investigated under optimum conditions using the model reaction/substrates **1a**. Upon reaction completion, the product was extracted from the catalyst 40MoAl200 by adding a minimum amount of organic solvent under ball milling (150 rpm, 5 min) toward optimum dissolution. Afterwards, the liquid phase taken from the reactor was then evaporated under reduced pressure to furnish the pure product **2a** in 96% isolated yield (Table 7, entry 1). The chamber of the ball mill containing the catalyst 40MoAl200 was then oven-dried (100°C, 10 min) and the solid catalyst recovered as a fine powder and reused in further runs. TGA analysis of the recovered catalyst was performed (200 °C, 2 h, air) showing no significant loss of weight (see Figure S2). The reused catalyst 40MoAl200 exhibited a stable and comparable efficiency to the fresh catalyst over three consecutive runs. After the three reuse cycles, 40 MoAl200 was recovered and its structure was further characterized by XRD, TEM, BET analyses in order to study the influence of the mechanical and chemical stress after subsequent reactions on the catalyst features.

Table 7. Recovery and reuse experiments of 40MoAl200 in the mechanochemical oxidation of diphenyl sulfide

Entry	Run	Conversion (%)[a]	Selectivity (**2a**)/(**3a**)[b]	Yield (%mol)
1	I	99	9.95:0.05	96
2	II	99	9.95:0.05	95
3	III	95	9.5:0.5	92

[a] Monitored by GC analyses; [b] Determined by GC-MS analyses. Reaction conditions: 25 stainless steel mL jar containing 8 balls (Ø 10 mm), 0.043 %mol 40MoAl200, (**1a**)/ H_2O_2 1:1 molar ratio, 350 rpm, 15 min.

The characterization analyses have been included as part of the Supporting Information, clearly demonstrating that the recovered catalyst maintained its crystallinity, particle size (31.25 nm by Scherrer equation based on characteristic 2θ 28.173) and morphology (Figures S3, S4). Textural properties did not show any relevant changes as compared to the fresh catalyst (Figure S5, Table S6) EDX, ICP and the acidity analyses (see Table S7-8) additionally confirmed the stability of the catalyst during the repeated reaction runs and no relevant leaching of phosphomolybdic acid was observed. Furthermore the mapping of 40MoAl200 (Figure S7) confirmed the retention of the homogeneous dispersion of HPA over CATAPAL200.

CONCLUSIONS

In conclusion, we have reported a detailed study on the preparation and use of 40MoAl200 as heterogeneous catalyst under Liquid assisted grinding (LAG) conditions for the selective oxidation of organic sulfides to sulfoxides. The catalyst was proved to be highly efficient, showing excellent results in terms of conversions and selectivity. Several parameters including the influence of the mechanochemical energy milling speed, number of milling balls and time were investigated and confirmed to be crucial parameters for the application of this technology in the use of

heterogeneous catalysts. Most importantly, the protocol could be scaled up 20 times (from 1 mmol to 20 mmol scale reagents) to achieve quantitative conversion and selectivity (both >99%) to products with the possibility of product isolation (isolated product yields in the 90-97% range). Several sulfide substrates were tested and successfully oxidized under LAG mechanochemical conditions, demonstrating the versatility of the developed protocol. The reusability of the catalyst was also successfully accomplished, confirming that the mechanochemical approach does not influence the crystallinity, surface and/or textural properties of the catalyst under the investigated optimum reaction conditions. The LAG protocol developed could be considered efficient, versatile, sustainable and suitable for preparative applications, with the potential to be scaled up for the synthesis of relevant organic compounds (i.e. pharmaceutical intermediates).

ACKNOWLEDGMENTS

The Università degli Studi di Perugia and MIUR are acknowledged for financial support to the project AMIS, through the program "Dipartimenti di Eccellenza - 2018-2022". GPR and AGS thanks for the financial support of CONICET through the "Becas Externas" program and UNLP. RL gratefully acknowledges support from MINECO under project CTQ2016-78289-P, co-financed with FEDER funds. The publication has been prepared with support from RUDN University Program 5-100.

REFERENCES

[1] A. D. McNaught, A. Wilkinson in *IUPAC Compendium of Chemical Technology (the "Gold Book")*, Blackwell Scientific Publication, Oxford, 2nd, **1997**.

[2] S. Immohr, M.Felderhoff, C. Weidenthaler, F. Schüth, *Angew. Chem. Int. Ed.* **2013**, 52, 12688-12691.

[3] Z. V. Todres, Organic Mechanochemistry and its Practical Applications, Taylor & Francis, Boca Raton, **2006**.

[4] K. Tanaka, Solvent-free Organic Synthesis, Wiley-VCH, Weinheim, 2nd Ed. **2008**.

[5] B. Ranu, A. Stolle, G. Kraus in *Ball Milling Toward Green Synthesis: Applications, Project, Challenges,* Royal Society of Chemistry, United Kingdom, **2014**.

[6] J. Howard, Y. Sagatov, L. Repusseau, C. Schotten, L. Duncan, D. Browne, *Green Chem.* **2017**,*19*, 2798-2802.

[7] A. Stolle, T. Szuppa, S. Leonhardt, B. Ondruschka, *Chem. Soc. Rev.* **2011,** *40***,** 2317-2329.

[8] A. Barakat, C. Mayer-Laigle, A. Solhy, R. Arancon, H. de Vries, R. Luque, *RSC Adv*. **2014**, *4*, 48109-48127.

[9] T. Friscic, *J. Mater. Chem*. **2010**, 20, 7599–7605.

[10] A.L. Garay, A. Pinchon, S.L. James, *Chem. Soc. Rev*. **2007**,36, 846–855.

[11] F. Mangin, P. Prinsen, A. Yepez, M.R. Hassan, S. Giliani, G. Xu, C. Len, R. Luque, *Catal. Comm*. **2018**, 104, 67-70.

[12] W. Ouyang, E. Kuna, A. Yepez, A.M. Balu, A. Romero, J.C. Colmeranes, R. Luque, *Nanomaterials* **2016**, 6, 93-98.

[13] D. Rodriguez-Padron, A. Puente Santiago, A. Benitez, A. Caballero, A.M. Balu, A. Romero, R. Luque, *J. Mater. Chem. A.* **2017**, 5, 16404-1641.

[14] A. Franco, S. De, A.M. Balu, A. Garcia, R. Luque, *Beilstein J. Org. Chem.* **2017**, 13, 1439-1445.

[15] A. Pineda, A.M. Balu, J. M. Campelo, A. Romero, D. Carmona, Balas, F. J. Santamaria, R. Luque, *ChemSusChem* **2011**, 4, 1561-1566.

[16] W. Yuan, T. Friscic, D. Apperly, S.L. James, *Angew. Chem. Int. Ed*. **2010**, 49, 3916-3919.

[17] M. Lanzillotto, L. Konnert, F. Lamaty, E. Colacino, *ACS Sustainable Chem. Eng.* **2013**, 1, 1196-1191.

[18] J. Mokhatari, M.R. Naimi-Jamal, H. Hamzeali, M.G. Dekamin, G. Kaupp, *ChemSusChem.* **2009**, 2, 248-254.

[19] D.C. Waddel, I. Thiel, A. Bunger, D. Nkata, A. Maloney, T. Clarks, B. Smith, J. Mack, *Green Chem*. **2011**, 13, 3156-3161.

[20] E. Colacino, P. Nun, F. M. Colacino, J. Martinez, F. Lamaty, *Tetrahedron* **2008**, 64, 5569-5576.

[21] D.C. Waddell, I. Thiel, T.D. Clarks, S.T. Marcum, J. Mack, *Green Chem.* **2010**, 12, 209-211.

[22] N. Mukherjee, T. Chatterjee, B. C. Ranu, *J. Org. Chem*. **2013**, 78, 11110-11114.

[23] T. Friscic, A. V. Trask, W. Jones, W. D. S. Motherwell, *Angew. Chem. Int. Ed*. **2006**, 20, 7546-7550.

[24] R. Thorwirth, A. Stolle, B. Ondruschka, *Green Chem*. **2010**, 12, 985-991.

[25] J. Galvez, M. Galvez-Llompart, R. Garcia- Domenech, *Green Chem.* **2010**, 12, 1056-1061.

[26] V. Declerck, E. Colacino, X. Bantreil, J. Martinez, F. Lamaty, *Chem*. *Commun*. **2012**, 48,11778-11780.

[27] A. Bruckmann, A. Krebs, C. Bolm, *Green Chem*. **2008**, 10, 1131-1141.

[28] W. C. Shearouse, J. Mack, *Green Chem*. **2012**, 14, 2771-2775.

[29] T.J. Sommer, *Tetrahedron Lett*. **2013**, 54, 2344-2347.

[30] R. Scmidt, A. Stolle, B. Ondruschka, W. Hope, *Green Chem*. **2012**, 14, 1673-1679.

[31] T. Szuppa, A. Stolle, W. Hope, *ChemSusChem*. **2012**, 3, 1181-1192.

[32] T. Szuppa, A. Stolle, B. Ondruschka, *Green Chem*. **2010**, 12, 1288-1292.

[33] J. Gao, G. Wang, *J. Org. Chem*. **2008**, 73, 2955- 2963.

[34] F. Fringuelli, F. Pizzo, L. Vaccaro *J. Org. Chem.* **2004**, *69*, 2315–2321.

[35] D. Amantini, F. Fringuelli, F. Pizzo, S. Tortoioli, L. Vaccaro, *Synlett.* **2003**, 348, 2292-2296.

[36] C.K. Hazra, Q. Dherbassy, J. Wencel-Delord, F. Colobert, *Angew. Chem. Int. Ed.* **2014**, 53, 13871- 13875.

[37] G. Fioroni, F. Fringuelli, L. Pizzo, L. Vaccaro *Green Chem.*, **2003**, *5*, 436–440.

[38] G. Cravotto, D. Garella, D. Carnaroglio, C. Gaudino, O. Rosati, *Chem. Commun*. **2012**, 48, 11632-11634.

[39] M. Aghajani, E. Safei, B. Karimi, *Synthetic Metals*, **2017**, 233, 63-73.

[40] F. Alamdari, R. Zekri, N. Jamali, A. R. Farsani, *Catal. Commun*. **2017**, 98, 71-75.

[41] M. Amini, M.M. Najafpour, S. Salimi, S. Ramezani, F. Ashouri, G. Mahmoudi, *Appl. Organomet. Chem*. **2017**, 31, 3892-3902.

[42] N. Afzali, S. Tangestaninejad, M. Moghadam, V. Mirkhani, A. Mechler, I.M. Baltork, V. Kardananpour, F. Zadehahmadi, *Appl Organometal Chem*. **2018**, 32, 3958-3969.

[43] E. Badetti, A. Bonetto, F. Romano, L. Marchiò, C. Zonta, G. Licini, *Catal. Lett*. **2017**, 146, 2312-2325.

[44] R. Frenzel, A. Sathicq, B. Gustavo, P. Romanelli, L. P. Pizzio, *J. Mol. Catal. A: Chem*. **2015**, 403, 27-36.

[45] L. Frattini, A. Isaacs, C. Parlett, K. Wilson, G. Kyriakou, A.F. Lee, *Appl. Catal. B: Env*. **2017**, 200, 10-18.

[46] T. Okuhara, N. Mizuno, M. Misono, *Applied Catal*. A **2001**, 222, 63-77.

[47] Y. Zhou, Y. Chen, Z. Long, J. Wang. *RSC Adv*. **2014**, 4, 42092-42113.

[48] M. Nuchter, N. Ondruscka, R. Trotzky, *J. Prakt. Chem*. **2000**, 342, 720- 728.

[49] Z. Zhang, W. Dong, G. Wang, K. Komatsu, *Synlett*. **2004**,1, 61-64.

[50] A. Ghorbani-Choghamarani, B. Tahmasbi, *New. J. Chem*. **2016**, 40, 1205-1211.

[51] H. Liu, J. Deng, W. Li, *Catal. Lett. **2010**,* 137, 261-264.

[52] K. Bahrami, M.M. Khodaei, M. Roastei, *New. J. Chem*. **2014**, 38, 5515-5520.

[53] E. Carbonell, E. Delgado-Pinar, J. Pitarch-Jarque, J. Alarcon, E. Garcia- Espana, *J. Phys. Chem. C*, **2013,** 117, 14325-14331.

[54] M. Haiiami, A. Ghorbani-Choghamarani, R. Ghafouri- Nejad, B. Tahmasbi, *New J. Chem*., **2016**, 40, 3066-3070.

[55] G. Paglia, C.E. Buckley, A.L. Rohl, R.D. Hart, K. Winter, A.J. Studer, B.A. Hunter, J.V. Hanna, *Chem. Mater.* **2004**, 16, 220-236.